http://dx.doi.org/10.5935/0103-5053.20140034

J. Braz. Chem. Soc., Vol. 25, No. 3, 579-588, 2014.
Printed in Brazil - ©2014 Sociedade Brasileira de Química
0103 - 5053 $6.00+0.00

Article

Decoration of Ti/TiO_2 Nanotubes with Pt Nanoparticles for Enhanced UV-Vis Light Absorption in Photoelectrocatalytic Process

Lucio C. Almeida* and Maria V. B. Zanoni

Departamento de Química, Instituto de Química, Universidade Estadual Paulista Júlio Mesquita Filho (UNESP), Rua Francisco Degni, 55, Bairro Quitandinha, 14800-900 Araraquara-SP, Brazil

Nanotubos de TiO_2 (TiO_2NTs) foram decorados com nanopartículas de Pt via deposição catódica. Estas nanopartículas foram uniformemente distribuídas, altamente separadas e espaçadas sobre toda a superfície do TiO_2NT para o menor tempo de deposição, com os tamanhos das partículas de Pt proporcionais às cargas aplicadas. O fotoeletrodo de Pt/TiO_2NTs apresentou intenso pico de absorção na região do visível com significativo deslocamento para vermelho induzido pela platina depositada na superfície do TiO_2NTs, diminuindo a energia do band gap de 3,21 eV para 2,87 eV. O fotoeletrodo de Pt/TiO_2NTs foi testado na oxidação fotoeletrocatalítica do corante Vermelho Ácido 29 com grande sucesso. Descoloração total e 92% de remoção do carbono orgânico total foram obtidos após 120 min de tratamento empregando o fotoeletrodo de Pt/TiO_2NTs, o qual apresentou valores superiores aos do não-decorado (87% e 68%, respectivamente), devido ao melhor uso da radiação e da minimização da recombinação de carga.

Pt nanoparticles were decorated on TiO_2 nanotube arrays (TiO_2NTs) by cathodic deposition. These nanoparticles were uniformly distributed, highly separated and spaced all over TiO_2NT surface to shorten deposition times with Pt particle sizes proportional to the applied charges. The Pt/TiO_2NT photoelectrode shows an intense absorption peak in the visible region with a significant red shift induced by Pt deposited on TiO_2NT surface, decreasing the band gap energy from 3.21 eV to 2.87 eV. Pt/TiO_2NT photoelectrode was tested as photoanode in the photoeletrocatalytic oxidation of Acid Red 29 dye with great success. Total decolorization and 92% of total organic carbon removal were obtained after 120 min of treatment by using Pt/TiO_2NT photoelectrode which was superior to the values obtained for the undecorated one (87% and 68%, respectively) due to better use of irradiation and minimization of charge recombination.

Keywords: photoelectrocatalytic process, Pt decorated TiO_2, dye degradation

Introduction

The exponential increase of industrial activities and the high demand for manufactured products have caused a considerable impact on the environment. In this context, new environmentally friendly techniques to eliminate or at least reduce the effect of recalcitrant pollutants have been developed.[1-5] Among the different techniques employed for contaminant removal, electrochemical advanced oxidation processes (EAOPs) have aroused a great interest for degradation/mineralization of organic pollutants due to their potential environmental compatibility,[6] since it rears no generation of secondary pollution, and allows the use of biologically inert materials and of low cost without generation of secondary pollution. Moreover, the EAOPs are being widely studied because of the strongly oxidant hydroxyl radical (•OH) generation which reacts non-selectively with organic compounds in waters.[7]

Among the different EAOPs, photoelectrocatalysis by using semiconductor materials has been extensively investigated in recent decades, with emphasis on the semiconductor TiO_2.[4,8-10] The combination of bias potential and UV irradiation has contributed to many applications, such as wastewater treatment.[2,4,11-14] Although many studies reported in literature have demonstrated the efficiency of TiO_2 as photoanode for degradation/oxidation of persistent organic compounds,[12-14] the interest of improving the properties of this material with focus on decreasing the high band gap value (3.20 eV) for TiO_2 in anatase phase,[15-17] which limits its photoactivity at low wavelengths,[16] has gained attention.

*e-mail: luciobonn@yahoo.com.br

The doping or band gap engineering of TiO_2 has been made in order to shift the absorption spectra to longer wavelengths. This is obtained by the incorporation of metal ions into the lattice, such as Pt,[18,19] non-metals such as C and N[20,21] and composites of semiconductors such as WO_3/TiO_2.[22]

Platinum decorated TiO_2 nanotubes (Pt/TiO_2NTs) have been destined for methanol, glucose and dopamine oxidation.[23-26] The introduction of Pt nanoparticles on TiO_2NTs (undecorated) has improved its electrical conductivity, catalytic activity and its stability in several chemicals.[27-29] Furthermore, the properties of this metal may also favor the enhancement of organic compound degradation (i.e., enhancement of the photocatalytic efficiency), since the Fermi levels of these metals are lower than the TiO_2NT conduction band when deposited on this material, allowing the electrons to move towards the noble metal Fermi levels, reducing the electron-hole recombination rate.[30-32] The decrease in electron density within the TiO_2NTs causes the holes which freely diffuse to the surface where oxidation of organic compounds can occur.

Park *et al.*[33] deposited Pt nanoparticles on the TiO_2NT structure by photoreduction method and their physicochemical properties were investigated. In this work, Pt decorated photoelectrode exhibited higher photocatalytic performance than the undecorated one on the photodegradation of Methylene Blue dye. Pt/TiO_2NT photoelectrodes prepared by platinum deposition-precipitation method were also studied by Zhu *et al.*[34] and their photocatalytic performance was evaluated by the degradation rates of Methyl Orange solution under UV-vis light irradiation. Using stable TiO_2NTs, An *et al.*[35] studied the Pt nanoparticle deposition on nanotubular TiO_2 surface via photodeposition process and the photocatalytic performance was also evaluated by the photodegradation of Methyl Orange under UV light irradiation. According to these authors, Pt/TiO_2NTs exhibited higher photocatalytic activity than the undecorated one. Hosseini and Momeni[36] recently evaluated the performance of Pt/TiO_2NT electrodes for electrochemical oxidation of formic acid. Nevertheless, the literature does not explore the increase of electrical conductivity of Pt/TiO_2NTs to evaluate its performance in the photoelectrocatalytic oxidation of an organic pollutant.

In this context, the present work reports the preparation of Pt/TiO_2NT photoelectrodes by galvanostatic electrodeposition of Pt nanoparticles on TiO_2NT surface. The influence of Pt introduction onto TiO_2NT surface was evaluated by systematic characterization of the morphology and photoactivity response when irradiated by UV-Vis light. In order to assess the photoelectrocatalytic (PEC) performance of the Pt/TiO_2NT photoelectrode, this material was applied to the degradation of the azo dye Acid Red 29 (AR29) (see formula in Figure 1). This textile dye was chosen as model compound due to its wide applicability and because 70% of the dyes usually consumed in the world are based on azo dyes, characterized by the presence of one or more azo groups (–N=N–).[3,37] Percentages of color removal and changes of total organic carbon (TOC) of AR29 dye solutions were monitored as responses. Decay kinetics for AR29 dye was followed by high-performance liquid chromatography (HPLC) during the dye mineralization. All results are compared with TiO_2NTs without modification.

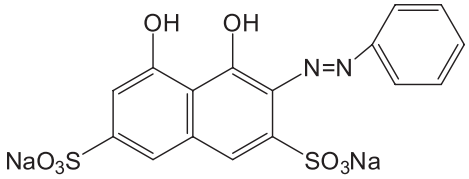

Figure 1. Molecular formula for acid red 29 (AR29) azo dye. Color index number: 16570.

Experimental

Preparation of TiO_2NT and Pt/TiO_2NT photoelectrodes

TiO_2NT electrodes were produced by anodization according to described in the literature.[2,38] For this, titanium sheets (99.9%, Sigma Aldrich) were previously cut (2.0 cm × 2.5 cm) and mechanically polished with different sandpapers, ultrasonically degreased in isopropyl alcohol, acetone and ultrapure water, successively for 15 min each one and drying in nitrogen flow. The TiO_2NT photoelectrodes were prepared by anodization using two-electrode cell configuration, with Ti foils as anode and ruthenium foil (2.0 cm × 2.0 cm) as a cathode. Ethylene glycol solution containing 0.25 wt.% NH_4F and 10 vol.% ultrapure water was used as electrolyte. The anodization consisted of a potential ramp from 0 to 30 V (sweep rate of 1.0 V min^{-1}) maintained at a constant potential of 30 V for 50 h. Immediately after the anodization the obtained electrodes were fired at 450 °C during 30 min in a muffle furnace to transform amorphous TiO_2 into crystalline anatase phase.

Finally, Pt/TiO_2NT photoelectrodes were prepared by Pt nanoparticle deposition on TiO_2NT surface by using a procedure adapted from Hosseini *et al.*.[39] A conventional three-electrode electrochemical cell with a platinum gauze (auxiliary electrode) and Ag/AgCl (reference electrode) was used for deposition of Pt nanoparticles on TiO_2NTs. All the Pt electrodeposition assays were performed at cathodic current density of 10 mA cm^{-2} in 10 mmol L^{-1} chloroplatinic

acid (≥ 99.9% purity, Sigma Aldrich) of ethanolic solution and at room temperature. In this electrochemical method, deposition times of 15, 20, 30 and 40 min were studied and a potentiostat/galvanostat (AUTOLAB Model PGSTAT 302) controlled by GPES software was used during the electro deposition experiments.

Characterization of the Pt/TiO_2NT photoelectrodes

TiO_2NT (undecorated) and Pt/TiO_2NT photoelectrodes were characterized according to their physical structure by means of X-ray diffraction (XRD) on a Siemens D 5000 using radiation in the 4 to 70° range. The structures and morphologies were characterized by field emission gun scanning electron microscopy (FEG-SEM), Zeiss Supra 35, coupled to an energy dispersive X-ray (EDX). The photochemical properties were analyzed by diffuse reflectance spectroscopy (DRS), by using an UV/Vis/NIR spectrophotometer (PerkinElmer Lambda 1050) equipped with a 150 mm Integrating Sphere and a high sensitivity Gridless-PMT detector operating between 200 and 800 nm. The UV/Vis/NIR spectrophotometer was calibrated with a Spectralon standard (Labsphere USRS-99-020).

Photocurrent measurements of both photoelectrodes were performed with a Potentiostat/Galvanostat Model 263 (EG&G Princeton Applied Research Co., USA), by using a conventional three-electrode cell with a double jacket where external thermostated water recirculated to maintain the solution temperature at 25 °C. A Philips high-pressure Hg lamp (I = 9.2 W m^{-2} and 125 W) without glass protection (inserted in a quartz cylinder) was immersed in 250 mL of 0.100 mol L^{-1} aqueous sodium sulfate (Na_2SO_4). A platinum wire and an Ag/AgCl (KCl, 3.0 mol L^{-1}) were employed as counter and reference electrodes, respectively. The linear sweeps were carried out using a scan rate of 10 mV s^{-1}, in the range potential of –0.5 to 2.0 V under and without lamp exposure, separated from the photoanode by a distance of 2.0 cm.

Evaluation of the photoelectrocatalytic activities of TiO_2NT and Pt/TiO_2NT photoelectrodes

Photoelectrocatalytic experiments were performed by using a conventional three-electrode electrochemical cell with cylindrical cell of 500 mL capacity with a double jacket, where the temperature was maintained at 25 °C via external water recirculation by using a thermostat.

TiO_2NT (undecorated) and Pt/TiO_2NT photoelectrodes were used as anodes, platinum gauze as a cathode (auxiliary electrode) and Ag/AgCl (KCl, 3.0 mol L^{-1}) as the reference electrode. The geometric areas of the photoanodes were 5.0 cm^2, whereas the platinum gauze cathode was 4.0 cm^2. For all PEC experiments, photoanode and platinum gauze cathode were arranged around a high-pressure mercury lamp (125 W) without the bulb. The gap between photoanodes and Hg lamp was ca. 2.0 cm. The PEC assay experiments were performed with a TECTROL R3/AS1 power supply and under potentiostatic mode. The cell potentials were monitored with a MINIPA ET-2042D digital multimeter connected in parallel to the electrochemical cell.

Comparative PEC treatments (by using TiO_2NT and Pt/TiO_2NT photoelectrodes) of 500 mL of 85.4 mg L^{-1} AR29 solution (35 mg L^{-1} TOC) in 0.05 mol L^{-1} Na_2SO_4 were conducted at potential of 2.0 V *vs*. Ag/AgCl (KCl, 3.0 mol L^{-1}) in the range of pH from 3.0 to 6.0 and under continuous stirring with a magnetic bar to provide the transport of species towards the electrodes. Samples were withdrawn from the cell at regular time intervals. The color removal of AR29 solutions was monitored from the absorbance decay at the wavelength of 508 nm (corresponding to maximum absorption) using a Hewlett Packard 8453 UV-Vis spectrophotometer operating in the range of 190-900 nm and the efficiency of dye decolorization was calculated as:[3]

$$\text{Decolorization /\%} = [(A_0 - A_t) / A_0] \times 100 \quad (1)$$

where A_0 and A_t are the maximum absorbance (λ = 508 nm) before and after irradiation, respectively.

The degradation of AR29 solutions was monitored from the abatement of their TOC, determined on a Shimadzu TOC-V CPN analyzer and reproducible TOC values with an accuracy of ± 2% were always found by injecting 800 µL samples to the TOC analyzer. Decay kinetics of AR 29 were followed by reversed-phase HPLC using a Shimadzu 10 Avp LC fitted with a Spherisorb ODS2 (5 µm, 150 mm × 4.6 mm i.d.) column and coupled with photodiode array detectors at λ = 508 nm. The mobile phase used in isocratic mode was 75:25 (v/v) acetonitrile/phosphate buffer (pH = 3.5) with a flow rate of 0.6 mL min^{-1} at 25 °C.

Results and Discussion

Characterization of TiO_2NT and Pt/TiO_2NT photoelectrodes

Figures 2a-2e illustrate the morphologies of TiO_2NT photoelectrodes produced via anodization of Ti sheets before (Figure 2a) and after (Figures 2b-e) modification with Pt nanoparticles by electrodeposition methodology using different deposition times. The results indicate that the adopted methodology promoted the formation/growth of highly ordered and structured nanotubes, with

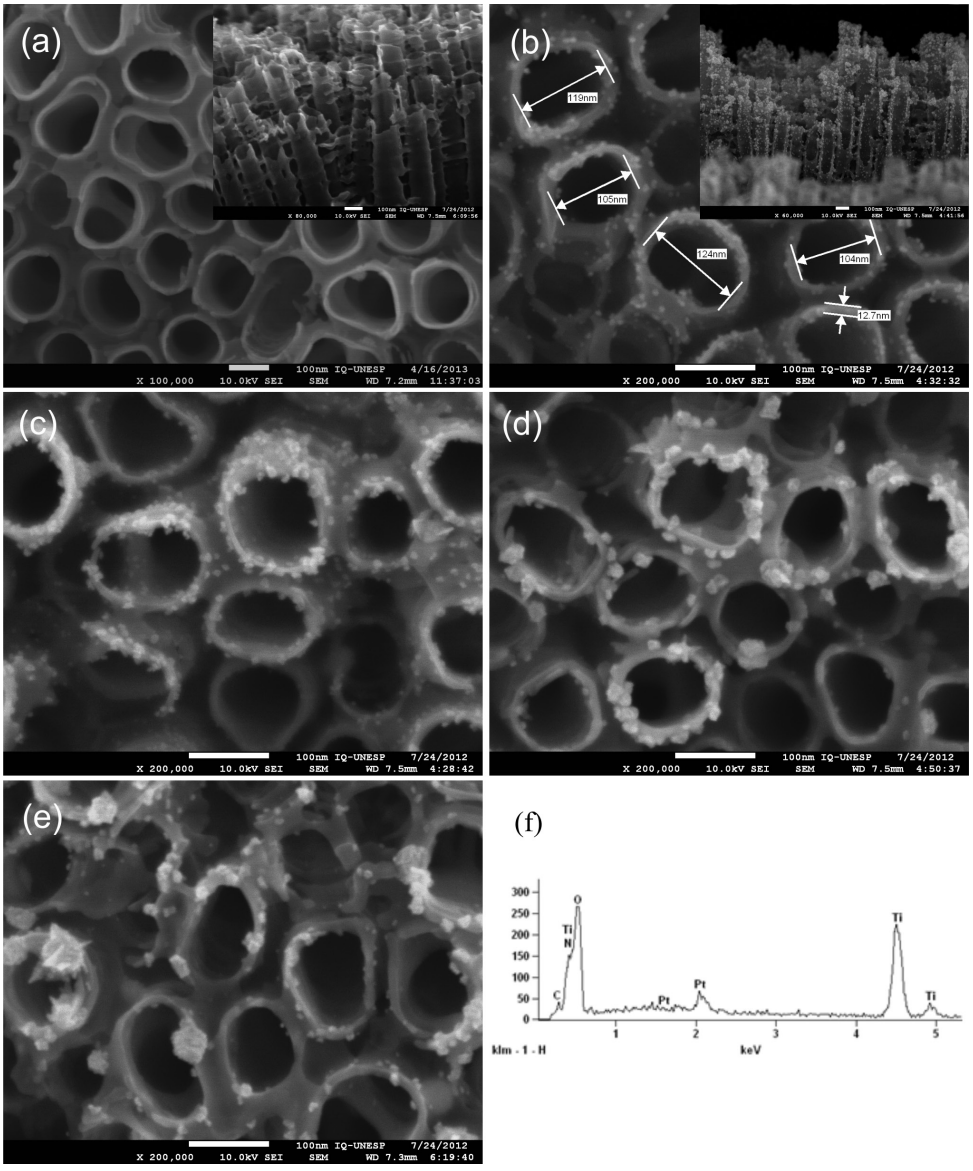

Figure 2. FEG-SEM image of (a) TiO_2NT (undecorated) and Pt/TiO_2NT photoelectrodes obtained at (b) 15 min, (c) 20 min, (d) 30 min and (e) 40 min of Pt electrochemical deposition. Inset of Figure 2a: cross-sectional view of the ordered TiO_2NT photoelectrode. Inset of Figure 2b: cross-sectional view of the ordered Pt/TiO_2NT (decorated) photoelectrode. (f) EDX graphic of ordered TiO_2NT decorated with Pt nanoparticles after 15 min of Pt electrodeposition.

mean inner diameters varying from 104 to 124 nm and with thickness of about 13 nm (see Figures 2a and 2b). The synthesized TiO_2NTs were remarkably well-aligned (vertically to the Ti substrate) with nanotube layers of up to 1.20 μm length, as shown in the inset of Figure 2a.

The Pt/TiO_2NT photoelectrodes prepared by electrochemical Pt deposition employing a cathodic current density of 10 mA cm^{-2} during 15, 20, 30 and 40 min (Figures 2b, c, d and e, respectively) show that the time of electrochemical reduction of chloroplatinic acid affects directly the Pt nanoparticles formation. By using 15 min of cathodic deposition the TiO_2NT surface is decorated with uniformly distributed Pt nanoparticles with diameter of 2-5 nm (Figure 2b), which were confirmed as Pt atoms by EDX measurements. The cross-sectional view illustrated at the inset of Figure 2b shows that the Pt nanoparticles were also uniformly deposited on TiO_2NT walls without any sign of aggregation, with nanoparticle sizes similar to those described above (2-5 nm). Figure 2c shows that Pt/TiO_2NT photoelectrode prepared employing 20 min of electrolysis presents deposits with bigger and more irregularly distributed Pt nanoparticles, with Pt deposits reaching up to 30 nm. Figures 2d and 2e (for 30 and 40 min of Pt deposition, respectively) indicated that the Pt deposits are deeply irregular with cluster formation, which compromises the deposits' quality. Furthermore, Pt/TiO_2NT electrodes obtained for 40 min of electrolysis showed Pt nanoparticles with varying sizes and poorly distributed Pt

clusters, when compared with the electrodes produced in shorter times (see Figure 2e). Therefore, we can verify that Pt particles sizes were proportional to the applied charge for electrodeposition, i.e., more aggregation of Pt nanoparticles was observed at longer deposition times. The results indicate that Pt deposition by electrochemical reduction on TiO_2NTs is very efficient for obtaining Pt nanoparticles regularly distributed on TiO_2NT surface, i.e., highly separated and spaced over all electrode surface, and short deposit times, such as 15 min can promote small particle formation and more efficient coating. Although EDX analysis has been used for all TiO_2NT photoelectrodes to confirm the formation and presence of platinum, for simplicity only EDX spectrum of Pt/TiO_2NT photoelectrode obtained during 15 min electrolysis is depicted, as can be seen in Figure 2f.

Figure 3 compares the X-ray diffraction patterns of the TiO_2NT and the Pt/TiO_2NT photoelectrodes (deposits of 15 min). As can be seen, the shape of X-ray diffraction peaks of Pt/TiO_2NT photoelectrode was similar to the undecorated one, due to the small Pt concentration in relation to the TiO_2NTs and to the detection limit of the equipment employed. All the diffraction peaks identified and located at 25.5, 38.1, 48.1, 54.8 and 62,7° are indexed as anatase TiO_2 (JCPDS card No. 21-1272) corresponding to reflections of (1 0 1), (0 0 4), (2 0 0), (1 0 5) and (2 0 4) planes, respectively.[35]

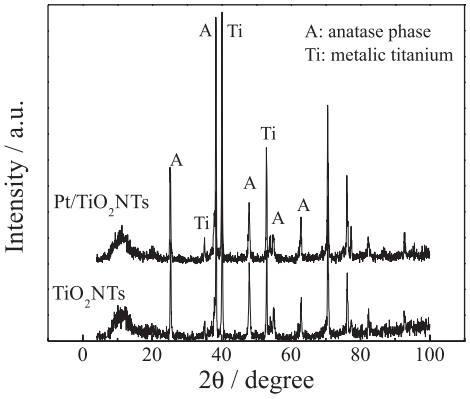

Figure 3. X-ray diffraction (XRD) patterns of TiO_2NT (undecorated) and Pt/TiO_2NT photoelectrodes before and after Pt nanoparticle deposition (for 15 minutes of Pt electrochemical deposition).

Photocurrent-potential curves in dark conditions (curve a) and under UV-Vis illumination by using TiO_2NT and Pt/TiO_2NT (Pt electrodeposition times of 15, 20, 30 and 40 min) photoelectrodes in 0.100 mol L^{-1} Na_2SO_4 are compared in Figure 4. All photocurrents generated for Pt/TiO_2NT (decorated) photoelectrodes (curves b-e, Figure 4) are higher than the undecorated one (Figure 4, Curve f), and gradually reaches current plateaus (saturated states) at positive potentials near 1.0 V under UV-Vis lamp exposure, with insignificant current response in the dark in the potential range of –0.5 to 2.0 V. Taking into consideration that the irradiation source includes UV and visible light content, it seems that the Pt introduction could be improving the light absorption in relation to TiO_2NTs (undecorated) that is activated only at wavelengths lower than 380 nm.

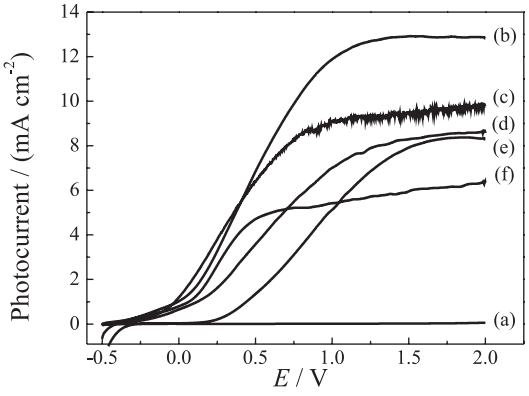

Figure 4. Photocurrent (linear sweep voltammetry) measurements obtained for Pt/TiO_2NT and TiO_2NT (undecorated) photoelectrodes at 10 mV s^{-1} and in 0.100 mol L^{-1} Na_2SO_4 in the absence of light (a) and under UV-Vis lamp exposure (b-f). Pt electrodeposition times: (b) 15 min, (c) 20 min, (d) 30 min and (e) 40 min. (f) TiO_2NT (undecorated) photoelectrode.

Nevertheless, comparing the effect of Pt nanoparticle size deposit on TiO_2NT surface it is possible to observe that the photocurrents generated were inversely proportional to the electrodeposition time. The maximum photocurrent densities for Pt/TiO_2NTs is obtained for Pt electrodeposition times of 15 min, approximately 41% higher than obtained for electrodeposition carried out on 40 min. The respective values of photocurrent (taken at 1.5 V) for all Pt/TiO_2NT (decorated in different times) photoelectrodes are shown in Table 1. This behavior can be simply explained by the formation of smaller and more uniformly distributed Pt nanoparticles which serve as efficient electron traps (i.e., Schottky barriers) to avoid the electro-hole recombination.[40] On the other hand, superfluous Pt content and/or a large particle size distribution on the TiO_2NT surfaces would block the transferring of electrons to the Pt nanoparticles to some extent, increasing the electron-hole recombination.[41] In short, the modification of TiO_2 with Pt smaller nanoparticles promotes efficient light absorption and reduction on the recombination of the photogenerated electron-hole pairs generated under UV-Vis light. These photogenerated holes can be trapped in the photoanode surface by H_2O/OH^- species, giving rise to $^{\bullet}OH$ radicals, which could improve the mineralization of organic compounds in favorable conditions.[5]

Table 1. Comparison of the results of photocurrent densities (I_{ph}) and Flat-band potentials (E_{fb}) for TiO_2NTs (undecorated) and Pt/TiO_2NTs (decorated in different times) in 0.100 mol L^{-1} Na_2SO_4 under UV irradiation exposure supplied by using a high-pressure mercury lamp (125 W) without the bulb

Photoelectrodes	[a]I_{ph} / (mA cm^{-2})	[b]E_{fb} / mV
TiO_2NTs (undecorated)	6.50	228
Pt/TiO_2NTs (15 min)	12.9	61
Pt/TiO_2NTs (20 min)	9.70	84
Pt/TiO_2NTs (30 min)	8.60	128
Pt/TiO_2NTs (40 min)	8.20	208

[a]At 1.5 V *vs.* Ag/AgCl; [b]flat-band potential *vs.* Ag/AgCl (KCl, 3.0 mol L^{-1}).

The other effect observed for photocurrent-potential curves by using TiO_2NT and Pt/TiO_2NT (Pt electrodeposition times of 15, 20, 30 and 40 min) photoelectrodes in 0.100 mol L^{-1} Na_2SO_4 (Figure 4) is the shift on flat-band potentials (E_{fb}). This corresponds to the situation in which there is no charge accumulation at semiconductors and that at n-type semiconductors photoanodic currents only flow at potentials more positive than E_{fb}.[42] The flat-band potentials for TiO_2NT (undecorated) and for all Pt/TiO_2NT photoelectrodes were calculated using the Butler equation,[5,43] and their values are exhibited in Table 1. From similar plots, the introduction of Pt nanoparticles promotes a shift of 167 mV in the flat-band potentials to less positive potential when TiO_2NTs are decorated with smaller Pt nanoparticles (electrochemical deposition during 15 min). This could be indicative of a better band bending and of a consequent improvement in the charge separation.[44]

These results are confirmed by comparing the UV-Vis diffuse reflectance spectra of TiO_2NTs (undecorated) and Pt/TiO_2NTs (electrodeposits of 15 min), as shown in Figure 5. The spectra indicates a strong light absorption in the UV region, ascribed to the charge transfer from the valence band (2p orbital of TiO_2NTs) to the conduction band (3d orbital of the Ti^{4+}) for both photoelectrodes.[45] But, marked peaks around 650 nm (absorption in the visible region) were observed for Pt/TiO_2NT materials. The increase in the absorption peak intensity in the visible region with the addition of platinum can possibly be related to surface plasmon resonance (SPR) effect of electrons in the Pt nanoparticles.[46,47] Additionally, it is observed a significant red shift induced by platinum deposited on TiO_2NTs probably due to the formation of an intra-gap energy level inside the band gap of TiO_2NTs.[46] Figure 6 shows the estimated band gap values (obtained by extrapolating the linear region to $(\alpha h\nu)^{1/2} = 0$) for TiO_2NT and Pt/TiO_2NT photoelectrodes, calculated with the Kubelka-Munk function (equation 2):[48]

$$\alpha\,(h\nu) = A\,(h\nu - E_g)^{n/2} \quad (2)$$

where α is the extinction coefficient, h is Planck's constant (J s), ν is the incident light frequency (s^{-1}), A is the absorption constant, E_g is the band gap (eV) and n is the absorption coefficient. An n value of 1 was chosen for all the samples, indicating a direct allowed optical transition.[49] The band gap of TiO_2NT (undecorated) and Pt/TiO_2NT photoelectrodes were estimated to be 3.21 and 2.87 eV, respectively (Figure 6). Thus, the results indicate that Pt deposition on TiO_2NT photoelectrode results in an increase in the visible-light response, i.e., that the deposition of Pt nanoparticles effectively extends the absorption from UV to a visible region by the reduction of the band gap value.[32] Taking into account that the irradiation system adopted as source promotes irradiation in UV and visible light, an improvement in the photodegradation of pollutants is expected when TiO_2NTs are decorated with Pt nanoparticles. Further studies were carried out comparing the degradation of AR29 dye by using both electrodes.

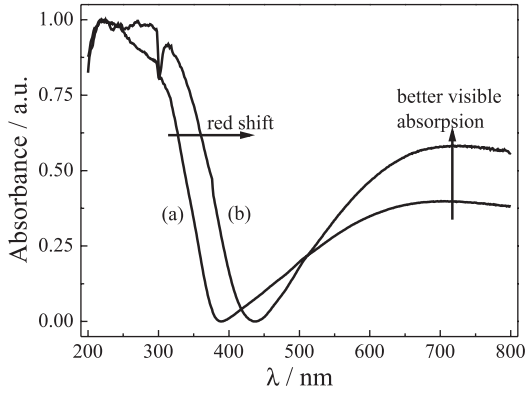

Figure 5. Diffuse reflectance spectra (DRS) of (a) TiO_2NT (undecorated) and (b) Pt/TiO_2NT (decorated with platinum by electrochemical deposition during 15 min) photoelectrodes.

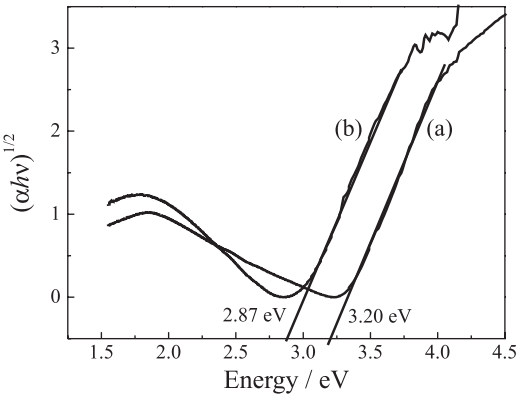

Figure 6. Plots of $(\alpha h\nu)^{1/2}$ *vs.* $h\nu$ employed to calculate the band gap values. Kubelka-Munk function $\alpha(h\nu) = A\,(h\nu - E_g)^{n/2}$ for (a) TiO_2NT (undecorated) and (b) Pt/TiO_2NT (decorated by electrochemical deposition during 15 min) photoelectrodes.

Degradation of AR29 dye at TiO_2NT and Pt/TiO_2NT photoelectrodes

In order to test the photoelectrocatalytic activities of TiO_2NT (undecorated) and Pt/TiO_2NT (decorated with Pt by electrochemical method during 15 min) photoelectrodes, PEC assays were conducted for 85.4 mg L^{-1} AR29 solutions (35 mg L^{-1} TOC) in 0.05 mol L^{-1} Na_2SO_4 (pH 6.0) at bias potential of 2.0 V *vs*. Ag/AgCl by using UV-Vis irradiation. Figure 7 compares the percentage of color removal and the TOC abatement obtained using TiO_2NT (undecorated) and Pt/TiO_2NT photoelectrodes. The percentage of decolorization was obtained by monitoring the absorbance at $\lambda = 508$ nm, where azo group is acting as chromophore.[3] As can be seen at Figure 7, PEC assays conducted by using Pt/TiO_2NT photoelectrode were more efficient than the undecorated one for both responses, i.e., for efficiency of decolorization and TOC abatement.

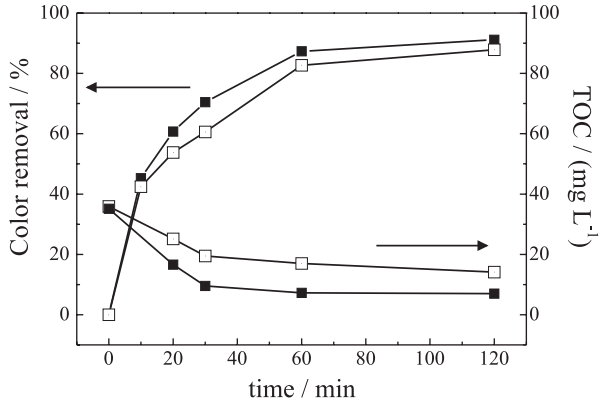

Figure 7. Percentage of color removal and TOC abatement *vs*. degradation time of 500 mL of a 85.4 mg L^{-1} Acid Red (AR29) solution in 0.05 mol L^{-1} Na_2SO_4 by the PEC process and applying 2.0 V *vs*. Ag/AgCl for: (□) TiO_2NT (undecorated) and (■) Pt/TiO_2NT (for 15 minutes of Pt electrochemical deposition) photoelectrodes. Applied pH: 6.0.

Then, the effect of pH was studied by monitoring the dye decolorization in 0.05 mol L^{-1} Na_2SO_4 at pH 3.0, 4.5 and 6.0, and bias potential of 2.0 V *vs*. Ag/AgCl by using UV-Vis irradiation. For all degradation experiments, slight pH decreases with prolonging electrolysis time up to 120 min were observed. This drop of pH can be related to the formation of aliphatic carboxylic acids as found for treatment of other dyes.[3,50] Taking into account that at acidic conditions there is no need of pH correction, all the experiments were done in acidic medium. The percentages of color removal calculated from equation 1 and for three pH values are plotted in Figure 8 for both photoelectrodes. Total color removal of the AR29 solutions was obtained by using the Pt/TiO_2NT (decorated) photoelectrode at pH values of 3.0 and 4.5 after 60 min of electrolysis. On the other hand, at pH 6.0 partial color removal (87%) was obtained for the same time of electrolysis. A similar tendency was observed while using TiO_2NT (undecorated) photoelectrodes, with maximum decolorization efficiencies at pH values of 3.0 and 4.5. However, decolorization efficiencies obtained by using the undecorated material were slightly lower compared to the decorated one for 60 min of electrolysis.

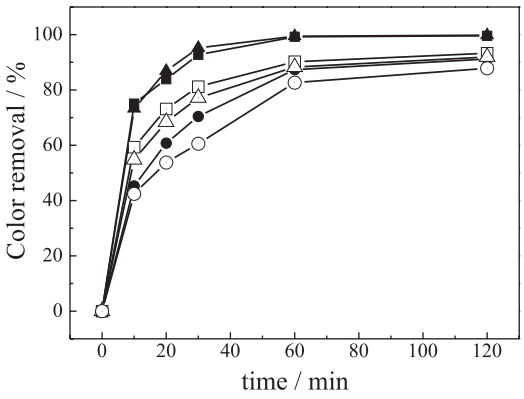

Figure 8. Effect of pH on color removal *vs*. degradation time of 500 mL of a 85.4 mg L^{-1} Acid Red (AR29) solution in 0.05 mol L^{-1} Na_2SO_4 by the PEC process and applying 2.0 V *vs*. Ag/AgCl for: (□, △, ○) TiO_2NT (undecorated) and (■, ▲, ●) Pt/TiO_2NT (for 15 minutes of Pt electrochemical deposition) photoelectrodes. Applied pH: (■, □) 3.0, (▲, △) 4.5 and (●, ○) 6.0.

The adsorption process of ionic form of the AR29 dye ($AR29^{2-}$) onto Pt/TiO_2NT and TiO_2NT surfaces is probably the first step in the process of AR29 oxidation.[51] So, the effect of pH on photoelectrocatalytic oxidation of AR29 may be securely explained by the relation/interaction between the surface charge of TiO_2 surface and the acid dissociation constant ($pK_a = -3.08$ at 25 °C) of AR29. Charge on TiO_2NT surface is formed by either protonation ($Ti–OH + H^+ \rightarrow Ti–OH_2^+$) or deprotonation ($Ti–OH + OH^- \rightarrow Ti–O^- + H_2O$) of the Ti–OH bonds.[52] It is known from literature that the isoelectric point (IEP) for TiO_2 varies between 5.2 and 5.5.[53] The IEP (or point of zero charge, PZC) is the pH at which the surface charge is electrically neutral. On the other hand, the surface is positively charged at a pH < IEP and negatively charged at pH > IEP.[52] The anionic form of the AR29 ($AR29^{2-}$) predominates above its pK_a value. Therefore, the pH range from –3.08 to 5.5 (i.e., at pH between the pK_a and the IEP) which may be the optimum condition for the adsorption of $AR29^{2-}$ onto Pt/TiO_2NT and TiO_2NT surfaces, explains why the kinetics of the AR29 oxidation was favored at more acid conditions. For pH values above 5.5 the TiO_2NT surface is negatively charged and the adsorption process of $AR29^{2-}$ is not favored.

Better results shown by the Pt/TiO_2NT photoelectrode compared with the undecorated one can be explained by

the fact that when coupling metallic Pt with TiO_2NTs, photogenerated electrons can flow from the semiconductor to the metallic Pt forming the Schottky barrier on the metal-semiconductor interface[33,35,54,55] due to the higher energy of conduction band of the TiO_2NTs (undecorated) compared with the new formed Fermi level of Pt/TiO_2NTs. So the electrons on the Pt surface can be transferred to adsorbed O_2 to form $O_2^{\bullet-}$, while holes accumulated at the valence band of TiO_2NTs led to the additional production of the strong and non-selective radical $^{\bullet}$OH. Finally, the hydroxyl radical formed reacts with the AR29 dye until their total mineralization, i.e., conversion into carbon dioxide, water and inorganic ions. In other words, Pt nanoparticles deposited on the TiO_2NT surface act as electron scavengers, promoting a better separation of electron-hole pairs. Consequently, more $^{\bullet}$OH radicals were generated, enhancing the photocatalytic activity of TiO_2NTs and the decolorization and degradation rates. Moreover, Pt/TiO_2NT photoelectrodes have shown a stronger light absorption both in UV and visible regions than that of undecorated ones (see Figure 8), which coincides with the absorption lines in the regions (i.e., at λ = 254, 373, 410, 441, 542 and 572 nm) obtained for the employed Hg lamp. Therefore, more photons with specific wavelength can be absorbed, thus enhancing the photoelectrocatalytic activity. Furthermore, AR29 solutions were exposed directly to the same high-pressure Hg lamp during 30 min and significant changes in the absorbance (at λ_{max} = 508 nm) were not observed, indicating that this dye is not directly photolyzed.

The mineralization of AR29 solutions by PEC process was monitored as a function of the TOC abatement. Figure 9 shows the TOC-time plots obtained for the degradation of the 85.4 mg L^{-1} AR29 solution by using TiO_2NT (undecorated) and Pt/TiO_2NT photoelectrodes at pH values of 3.0, 4.5 and 6.0. It can be observed that TOC decayed more rapidly for the Pt/TiO_2NT photoelectrode when compared to the undecorated one, after 120 min of degradation. At this time, TOC reductions of 92%, 89% and 80% were obtained for pH values of 3.0, 4.5 and 6.0, respectively. On the other hand, at the same time and by using the TiO_2NT (undecorated) photoelectrode only 66%, 67% and 61% of TOC abatement (after 120 min electrolysis) were found for pH values of 3.0, 4.5 and 6.0, respectively. These results corroborate the findings of photocurrent and decolorization obtained in this work (Figures 4 and 8, respectively), due to the better adsorption of ionic form of the AR29 dye ($AR29^{2-}$) onto Pt/TiO_2NT and TiO_2NT surfaces at more acid conditions (as explained above). As expected, higher efficiency on the dye mineralization was obtained by using the Pt/TiO_2NT material probably due to the better separation of electron-hole pairs generating additional $^{\bullet}$OH radicals, which accelerate the oxidation process, as it has been explained above. Furthermore, the TOC content in AR29 solutions did not vary when exposed to Hg lamp source during 120 min, confirming that the direct photolysis of this dye can be neglected. Although the decorated photoelectrode has yielded 92% TOC removal of dye solution, the formation of recalcitrant products (i.e., products hardly destroyed by photogenerated $^{\bullet}$OH radicals) may have prevented their total mineralization.[7]

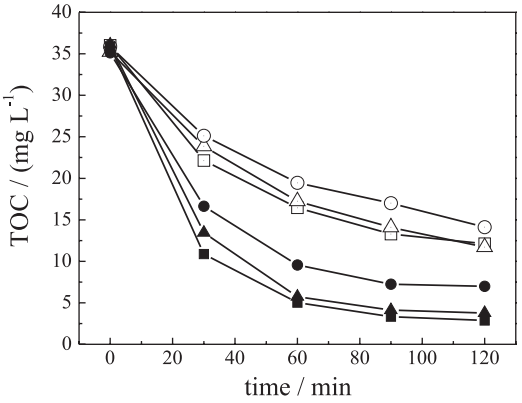

Figure 9. Effect of pH on TOC abatement *vs*. degradation time of 500 mL of a 85.4 mg L^{-1} AR29 solution (35 mg L^{-1} TOC) in 0.05 mol L^{-1} Na_2SO_4 by the PEC process and applying 2.0 V *vs*. Ag/AgCl for: (□, △, ○) TiO_2NT (undecorated) and (■, ▲, ●) Pt/TiO_2NT (for 15 min of Pt electrochemical deposition) photoelectrodes. Applied pH: (■, □) 3.0, (▲, △) 4.5 and (●, ○) 6.0.

The kinetics of degradation of 85.4 mg L^{-1} AR29 in 0.05 mol L^{-1} Na_2SO_4 by $^{\bullet}$OH radicals formed at Pt/TiO_2NT and TiO_2NT (undecorated) photoanode surfaces were also followed by reverse-phase HPLC coupled to diode array detector (see Figure 10). The chromatograms obtained for AR29 dye displayed a well-defined peak at retention time

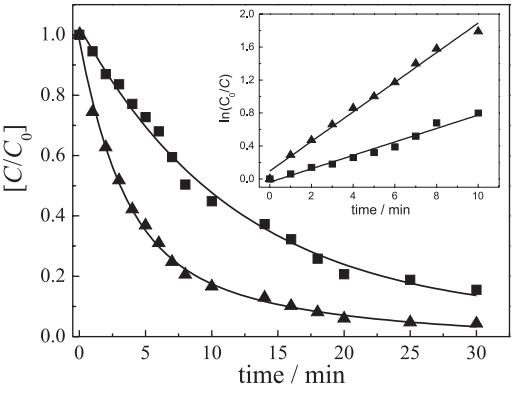

Figure 10. Decay of AR29 normalized concentration during the photoelectrocatalytic oxidation by using (■) TiO_2NT (undecorated) and (▲) Pt/TiO_2NT (for 15 minutes of Pt electrochemical deposition) photoelectrodes. Experimental conditions: potential of 2.0 V *vs*. Ag/AgCl (KCl, 3.0 mol L^{-1}) and pH 3.0. The inset panel presents the kinetics analysis considering pseudo first-order reactions for AR29 degradation.

(t_R) of 8.35 min. Direct photolysis of the AR29 dye was discarded because its content in solution remained constant after 120 min under UV lamp exposure and without potential application by the photoelectrochemical cell.

Figure 10 highlights the quick and almost total degradation of the 85.4 mg L^{-1} AR29 solution in 0.05 mol L^{-1} Na_2SO_4 at pH 3.0 by using Pt/TiO_2NTs (decorated) applying 2.0 V *vs*. Ag/AgCl and under UV-Vis irradiation exposure during 30 min. Similar concentration decay was observed using the TiO_2NT (undecorated) photoelectrode under the same experimental conditions. As can be seen in the inset in Figure 10, the concentration decays fitted well with equation expected for pseudo first-order kinetics. From this analysis, pseudo first-order constants (k_1) of 3.0 $\times$ 10^{-3} s^{-1} (R^2 = 0.996) and 1.36 $\times$ 10^{-3} s^{-1} (R^2 = 0.987) were obtained for Pt/TiO_2NT (decorated) and TiO_2NT photoelectrodes, respectively. The fastest AR29 dye degradation promoted by the Pt/TiO_2NT photoelectrode can be ascribed to Pt nanoparticles deposited on the TiO_2NT surface, which act as electron sinks promoting a better separation of electron-hole pairs, generating more •OH radicals,[32] and consequently also promoting a better light absorption than TiO_2NT (undecorated) photoelectrode.

These results are in agreement with the TOC abatement illustrated in Figure 9, indicating that the use of Pt/TiO_2NT photoelectrodes in the photoelectrocatalytic oxidation of dye are not only more efficient in decolorization of dye solutions, but also for TOC mineralization when compared to the undecorated one.

Conclusions

In this work, Pt decorated TiO_2NT photoelectrodes were prepared using different deposition times under galvanostatic condition. Platinum nanoparticles were more uniformly distributed, highly separated and spaced over the entire TiO_2NT surface in shorter deposition times. Additionally, it has been verified that Pt particle sizes were proportional to the applied charge, i.e., more aggregation (clusters) of Pt particles were observed at longer deposition times. Similarly, the higher photocurrent response was obtained by applying the Pt/TiO_2NT photoelectrode which presented a better Pt nanoparticle distribution on TiO_2NT surface. The band gap of this Pt/TiO_2NT photoelectrode was red shifted to the visible region in comparison with the undecorated one, and their band gap were estimated (by using Kubelka-Munk function) to be 3.21 and 2.87 eV, respectively.

The decolorization and mineralization rate of AR29 dye solutions were studied employing TiO_2NT (undecorated) and Pt/TiO_2NT photoelectrodes and at different pH values (3.0, 4.5 and 6.0). Although the total color removal of AR29 dye solutions has been achieved by using the Pt/TiO_2NT photoelectrode at pH values of 3.0 and 4.5 (i.e., pH values which are between the pK_a of AR29 and the IEP for TiO_2) after 60 min of electrolysis, at pH 6.0, only partial color removal (87%) was achieved at the same time. Similar tendency was observed for the undecorated photoelectrode, even if less efficient than the decorated one. Furthermore, TOC reductions of 66 and 92% were obtained at pH 3.0 (the optimum pH value) and after 120 min electrolysis by using TiO_2NT and Pt/TiO_2NT photoelectrodes, respectively. For both materials, the AR29 decay followed pseudo first-order kinetics with similar constant rates, which is double than with the Pt/TiO_2NTs electrode. This difference on TOC reductions showed that platinum nanoparticles improves the light absorption composed of UV and visible irradiation in relation to TiO_2NTs (undecorated) that is activated only by UV irradiation and, in addition, it can accelerate the dye mineralization due to the better separation of electron-hole pairs, generating additional •OH radicals, i.e., due to the higher photocatalytic activity of the Pt/TiO_2NT photoelectrode compared to the undecorated one. Finally, our results revealed that platinum modification of TiO_2NTs by using a simple method is a promising and an attractive way to develop photoelectrodes with high photocatalytic activity and capacity for dye oxidation improving the light absorption in a situation close to solar radiation.

Acknowledgements

The authors gratefully acknowledge the Brazilian research funding agencies CAPES, CNPq and FAPESP (Process: 2011/21606-9) for financial support.

References

1. Almeida, L. C.; Gasparotto, L. H. S.; Bocchi, N.; Rocha-Filho, R. C.; Biaggio, S. R.; *J. Appl. Electrochem*. **2008**, *38*, 167.
2. Brugnera, M. F.; Rajeshwar, K.; Cardoso, J. C.; Zanoni, M. V. B.; *Chemosphere* **2010**, *78*, 569.
3. Almeida, L. C.; Garcia-Segura, S.; Arias, C.; Bocchi, N.; Brillas, E.; *Chemosphere* **2012**, *89*, 751.
4. Paschoal, F. M. M.; Pepping, G.; Zanoni, M. V. B.; Anderson, M. A.; *Environ. Sci. Technol*. **2009**, *43*, 7496.
5. Guaraldo, T. T.; Pulcinelli, S. H.; Zanoni, M. V. B.; *J. Photochem. Photobiol., A* **2011**, *217*, 259.
6. Almeida, L. C.; Garcia-Segura, S.; Bocchi, N.; Brillas, E.; *Appl. Catal., B* **2011**, *103*, 21.
7. Garcia-Segura, S.; Almeida, L. C.; Bocchi, N.; Brillas, E.; *J. Hazard. Mater.* **2011**, *194*, 109.

8. Tacconi, N. R.; Rajeshwar, K.; *Electrochim. Acta* **2002**, *47*, 2603.
9. Khataee, A. R.; Safarpour, M.; Zarei, M.; Aber, S.; *J. Mol. Catal. A: Chem.* **2012**, *363-364*, 58.
10. Zhang, Y.; Xiong, X.; Han, Y.; Zhang, X.; Shen, F.; Deng, S.; Xiao, H.; Yang, X.; Yang, G.; Peng, H.; *Chemosphere* **2012**, *88*, 145.
11. Ferraz, E. R. A.; Oliveira, G. A. R.; Grando, M. D. T.; Lizier, M.; Zanoni, M. V. B.; Oliveira, D. P.; *J. Environ. Manag.* **2013**, *124*, 108.
12. Osugi, M. E.; Rajeshwar, K.; Ferraz, E. R. A.; Oliveira, D. P.; Araújo, A. R.; Zanoni, M. V. B.; *Electrochim. Acta* **2009**, *54*, 2086.
13. Oliveira, A. P.; Carneiro, P. A.; Sakagami, M. K.; Zanoni, M. V. B.; Umbuzeiro, G. A.; *Mutat. Res*. **2007**, *626*, 135.
14. Fraga, L. E.; Anderson, M. A.; Beatriz, M. L. P. M. A; Paschoal, F. M. M.; Romão, L. P.; Zanoni, M. V. B.; *Electrochim. Acta* **2009**, *54*, 2069.
15. Tang, H.; Prasad, K.; Sanjinès, R.; Schmid, P. E.; Levy, F.; *J. Appl. Phys*. **1994**, *75*, 2042.
16. Asahi, R.; Taga, Y.; Mannstadt, W.; Freeman, A. J.; *Phys. Rev. B: Condens. Matter* **2000**, *61*, 7459.
17. Elghniji, K.; Atyaoui, A.; Livraghi, S.; Bousselmi, L.; Giamello, E.; Ksibi, M.; *J. Alloys Compd.* **2012**, *541*, 421.
18. Sakthivel, S.; Shankar, M. V.; Palanichamy, M.; Arabindoo, B.; Bahnemann, D. W.; Murugesan, V.; *Water Res.* **2004**, *38*, 3001.
19. Xing, L.; Jia, J.; Wang, Y.; Zhang, B.; Dong, S.; *Int. J. Hydrogen Energy* **2010**, *35*, 12169.
20. Park, J. H.; Kim, S.; Bard, A. J.; *Nano Lett*. **2006**, *6*, 24.
21. Ghicov, A.; Macak, J. M.; Tsuchiya, H.; Kunze, J.; Haeublein, V.; Frey, L.; Schmuki, P.; *Nano Lett*. **2006**, *6*, 1080.
22. Guaraldo, T. T.; Zanoni, T. B.; de Torresi, S. I. C.; Gonçales, V. R.; Zocolo, G. J.; Oliveira, D. P.; Zanoni, M. V. B.; *Chemosphere* **2013**, *91*, 586.
23. Hosseini, M. G.; Momeni, M. M.; *Electrochim. Acta* **2012**, *70*, 1.
24. Song, Y. Y.; Gao, Z. D.; Schmuki, P.; *Electrochem. Comm*. **2011**, *13*, 290.
25. Hosseini, M. G.; Momeni, M. M.; *J. Solid State Electrochem.* **2010**, *14*, 1109.
26. Hosseini, M. G.; Monemi, M. M.; Faraji, M.; *J. Appl. Electrochem.* **2010**, *40*, 1421.
27. Hagfeldt, A.; Boschloo, G.; Sun, L.; Kloo, L.; Pettersson, H.; *Chem. Rev*. **2010**, *110*, 6595.
28. Zhang, W.; Minett, A. I.; Gao, M.; Zhao, J.; Razal, J. M.; Wallace, G. G.; Romeo, T.; Chen, J.; *Adv. Energy Mater*. **2011**, *1*, 671.
29. Wen, Z.; Wang, Q.; Li, J.; *Adv. Funct. Mater*. **2008**, *18*, 959.
30. Priya, R.; Baiju, K.; Shukla, S.; Biju, S.; Reddy, M.; Patil, K.; *Catal. Lett.* **2009**, *128*, 137.
31. Anandan, S.; Kumar, P. S.; Pugazhenthiran, N.; Madhavan, J.; Maruthamuthu, P.; *Sol. Energy Mater. Sol. Cells* **2008**, *92*, 929.
32. Wang, H.; Faria, J. L.; Dong, S.; Chang, Y.; *Mater. Sci. Eng. B* **2012**, *177*, 913.
33. Park, D. J.; Sekino, T.; Tsukuda, S.; Tanaka, S.; *J. Ceram. Soc. Jpn.* **2012**, *120*, 307.
34. Zhu, B.; Li, K.; Wang, S.; Zhang, S.; Wu, S.; Huang, W.; *J. Dispersion Sci. Technol.* **2008**, *29*, 1408.
35. An, H.; Zhou, J.; Li, J.; Zhu, B.; Wang, S.; Zhang, S.; Wu, S.; Huang, W.; *Catal. Commun.* **2009**, *11*, 175.
36. Hosseini, M. G.; Momeni, M. M.; *Fuel Cells* **2012**, *12*, 406.
37. Martínez-Huitle, C. A.; Brillas, E.; *Appl. Catal., B* **2009**, *87*, 105.
38. Cardoso, J. C.; Lizier, T. M.; Zanoni, M. V. B.; *Appl. Catal., B* **2010**, *99*, 96.
39. Hosseini, M. G.; Faraji, M.; Momeni, M. M.; *Thin Solid Films* **2011**, *519*, 3457.
40. Shan, Z.; Wu, J.; Xu, F.; Huang, F. Q.; Ding, H.; *J. Phys. Chem. C* **2008**, *112*, 15423.
41. Lai, Y.; Zhuang, H.; Xie, K.; Gong, D.; Tang, Y.; Sun, L.; Lin, C.; Chen, Z.; *New J. Chem*. **2010**, *34*, 1335.
42. Zanoni, M. V. B.; Sene, J. J.; Anderson, M. A.; *J. Photochem. Photobiol., A* **2003**, *157*, 55.
43. Butler, M. A.; *J. Appl. Phys*. **1977**, *48*, 1914.
44. Mukherjee, B.; Wilson, W.; Subramanian, V.; *Nanoscale* **2013**, *5*, 269.
45. Sobana, N.; Muruganadham, M.; Swaminathan, M.; *J. Mol. Catal. A: Chem*. **2006**, *258*, 124.
46. Wang, H.; Faria, J. L.; Dong, S.; Chang, Y.; *Mater. Sci. Eng., A* **2012**, *177*, 913.
47. Yang, Y.; Su, F.; Zhang, S.; Guo, W.; Yuan, X.; Guo, Y.; *Colloids Surf. A* **2012**, *415*, 399.
48. López, R.; Gómez, R.; *J. Sol-Gel Sci. Technol.* **2012**, *61*, 1.
49. Zhao, W.; Wang, Y.; Yang, Y.; Tang, J.; Yang, Y.; *Appl. Catal., B* **2012**, *115-116*, 90.
50. Salazar, R.; Garcia-Segura, S.; Ureta-Zañartu, M. S.; Brillas, E.; *Electrochim. Acta* **2011**, *56*, 6371.
51. Yang, S.; Liu, Y.; *Appl. Catal., A* **2006**, *301*, 284.
52. Kin, H. D.; Anderson, M. A.; *J. Photochem. Photobiol. A: Chem.* **1996**, *94*, 221.
53. Varghese, O. K.; Grimes, C. A.; *J. Nanosci. Nanotechnol*. **2003**, *3*, 277.
54. Linsebigler, A. L.; Lu, G.; Yates, J. J. T.; *Chem. Rev*. **1995**, *95*, 735.
55. Suwanchawalit, C.; Wongnawa, S.; Sriprang, P.; Meanha, P.; *Ceram. Int.* **2012**, *38*, 5201.

Submitted: October 22, 2013
Published online: February 11, 2014

FAPESP has sponsored the publication of this article.